JOURNAL OF MATERIALS SCIENCE 23 (1988) 4363–4368

Evaluation of the composition of reactively evaporated GeO$_x$ thin films from optical transmission and XPS data

J. BEYNON*, M. M. EL-SAMANOUDY*, E. L. SHORT‡
*Departments of *Physics and ‡Chemistry, Brunel University, Uxbridge, Middlesex, UK*

Computer simulations of germanium 3d core spectra obtained with reactively evaporated GeO$_x$ thin films ($0 \leqslant x \leqslant 2$) have been developed using a modified Sanderson approach, in which five basic sub-units are produced by the conversion of germanium atoms in the primary coordination sphere into either -GeO$_x$ groups or -OGeO$_x$ groups on oxidation. The relative proportion of the five sub-units are adjusted until the best agreement with the experimental XPS spectra is obtained. The volume fraction of germanium in GeO$_x$ obtained using an optical transmittance model is compared with the number fraction obtained from XPS data over a range of oxygen partial pressures.

1. Introduction

GeO$_x$ thin films have been prepared by reactively evaporating germanium in oxygen at various partial pressures. This preparation technique seems to have been pioneered by Birey [1] and used later by Demiryont and Tezey [2], amongst others, to study the electrical properties of Al$_x$O$_y$ thin films. Two approaches may be adopted for the depositions – either vary the partial pressure of oxygen whilst keeping the deposition rate constant or vary the deposition rate whilst keeping the oxygen partial pressure constant. In the present investigation the former method was always employed.

When characterizing the electrical and optical properties of thin films it is obviously essential for their composition to be determined. One method of achieving this aim is based on Birey's optical absorption model [1] which allows the volume percentage fraction of the metallic component in the thin film to be estimated. The second method, due to Takano *et al.* [3], models the XPS core spectra by first decomposing them into five components using a modified Sanderson electronegativity technique [4, 5] in order to obtain their binding energies. They used this technique with -GeO$_x$ thin films, prepared by RF sputtering of a sintered GeO$_2$ target in an argon–hydrogen gas mixture.

The purpose of the present investigation was threefold: to determine whether the XPS modelling procedure could also be applied to reactively evaporated thin films; to use a Basic program for use with a BBC Master microcomputer, to perform the calculations, in order to obtain optimal agreement between the experimental and simulated results; to correlate the results of the optical and XPS techniques.

2. Background

The optical model is based on the equivalence of a metal-oxide thin film, containing uniformly distributed metal particles, with a pure metallic thin film having the same optical absorption characteristics. The as-evaporated film, deposited on a substrate of refractive index n_s is illustrated in Fig. 1. It is assumed that the optically equivalent structure consists of a pure metallic film of reflectivity ϱ_m and transmissivity τ_m covered with pure metal-oxide which has a refractive index equal to the substrate.

If the interferometrically measured thickness of the deposited film is d_c and that of the equivalent metallic film is d_m, then the concentration of the metallic particles within the oxide is given by d_m/d_c.

The computer simulation procedure uses a modified Sanderson approach to follow the process by which germanium is oxidized to GeO$_2$. Metallic germanium has a primary coordination sphere consisting of four other germanium atoms, but as oxidation proceeds these atoms are converted into either -GeO$_x$ groups with retention of a Ge–Ge bond or -OGeO$_x$ groups into which an oxygen atom is inserted after a Ge–Ge

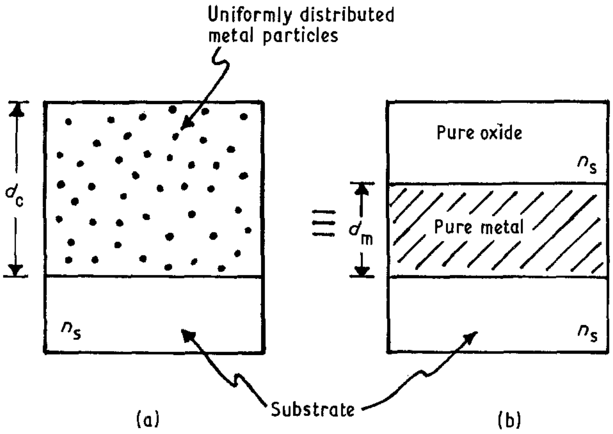

Figure 1 The evaporated thin film (a) with its optically equivalent structure (b).

0022-2461/88 $03.00 + .12

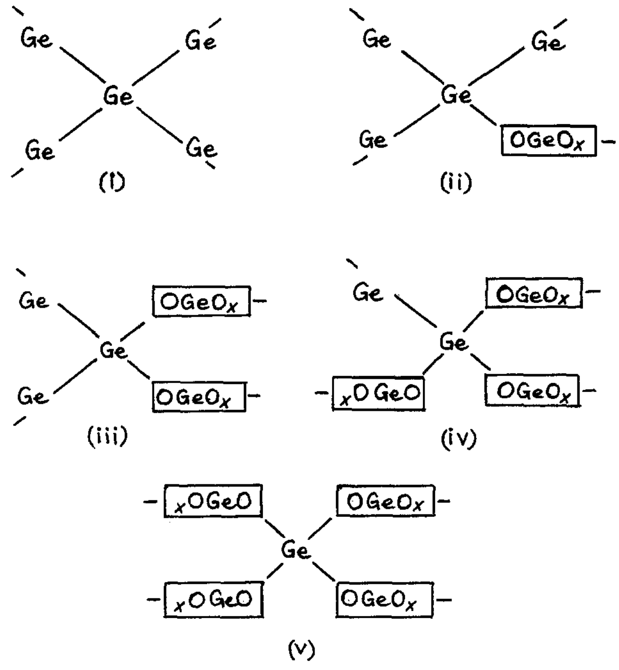

Figure 2 The five sub-units arising from oxidation of germanium atoms in the primary coordination sphere: (i) $Ge–Ge_4$, (ii) $Ge–Ge_3O$, (iii) $Ge–Ge_2O_2$, (iv) $Ge–GeO_3$, (v) $Ge–O_4$.

bond is broken. There are, therefore, five possible sub-units present in different proportions after the inception of oxidation. These are illustrated in Fig. 2. A germanium 3d core spectrum can be simulated if it is assumed that the spectrum is formed by the overlapping of five sub-peaks arising from the units (i) to (v) in Fig. 2. The binding energies of the sub-peaks can be calculated from electronegativity theory and their intensities by using the distribution probabilities for random bonding to form the five tetrahedra $Ge–Ge_xO_{4-x}$, where x equals 4 in germanium and zero in GeO_2.

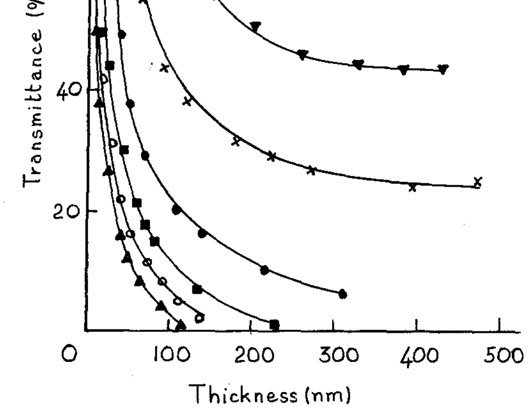

Figure 3 Variation of the optical transmittance with film thickness at various oxygen partial pressures for a wavelength of 600 nm: (▲) 1.0 mPa, (○) 6.0 mPa, (■) 20 mPa, (●) 40 mPa, (x) 70 mPa, (▼) GeO_2.

3. Experimental technique

Germanium and GeO_x thin films for optical study were deposited into Corning glass substrates, cleaned using conventional technique by reactive evaporation from a tungsten spiral basket in various partial pressures of oxygen (1.3–92.0 mPa). GeO_2 films were prepared by evaporation of GeO_2 powder from a molybdenum boat *in vacuo* at about 1.0 mPa. A range of thicknesses from 10 to 500 nm was used. Optical transmission spectra were obtained for a wavelength of 600 nm using a Perkin–Elmer Lambda 3 visible–UV spectrophotometer.

All specimens for the XPS investigation were prepared on mica substrates, and covered the same range of oxygen partial pressures as in the optical study. The spectrometer (Kratos Analytical Instruments Ltd, Model ES300) used AlKα radiation *in vacuo* at about 0.1 mPa and had a resolution of 0.95 eV. All measurements were carried out at "room" temperature, i.e. 298 K. The binding energy of the carbon C 1s state, namely 284.6 eV, was used as a reference for calibration purposes. A program (in Basic), written for the BBC Master microcomputer, enabled the binding energy of each of the five units shown in Fig. 2, as well as their relative amounts, to be calculated in 0.05 unit steps for values of x in the range $0 \leqslant x \leqslant 2$. The simulated XPS spectrum, drawn to the same scale as the XPS spectra, was obtained on a Watanabe A3 plotter. After comparing the experimental and simulated spectra, the parameters were varied until the optimum agreement was obtained.

4. Results

4.1. Optical

Fig. 3 shows the variation of the optical transmittance as a function of film thickness for a range of oxygen partial pressures. d_m is taken to be the thickness of the germanium film deposited at about 1.0 mPa, which has a transmittance of 45%. This is the minimum transmittance of the GeO_2 film. Similarly, d_c is the thickness of the GeO_x films deposited at the higher oxygen partial pressures. Hence Table I gives the values of the d_m/d_c ratios, and, hence, the metallic concentration V(Ge). It can be seen that as the oxygen pressure increases V(Ge) decreases, as is expected.

4.2. XPS

Fig. 4 depicts the XPS spectrum for a film deposited *in vacuo* at about 1.0 mPa. It can be seen that there is a residual oxygen peak. Hence the assumption made with the optical model cannot be fully justified. The germanium 3d peak consists primarily of an unresolved

TABLE I Concentration of germanium in GeO_x thin films prepared at different oxygen partial pressures

Oxygen partial pressure (mPa)	d_m (nm)	d_c (nm)	V(Ge) (%)
1.0	12.0	–	100
8.0	12.0	18.0	66.7
25.0	12.0	20.0	50.0
50.0	12.0	42.0	29.0
90.0	12.0	88.0	13.7
GeO_2	12.0	270	4.5

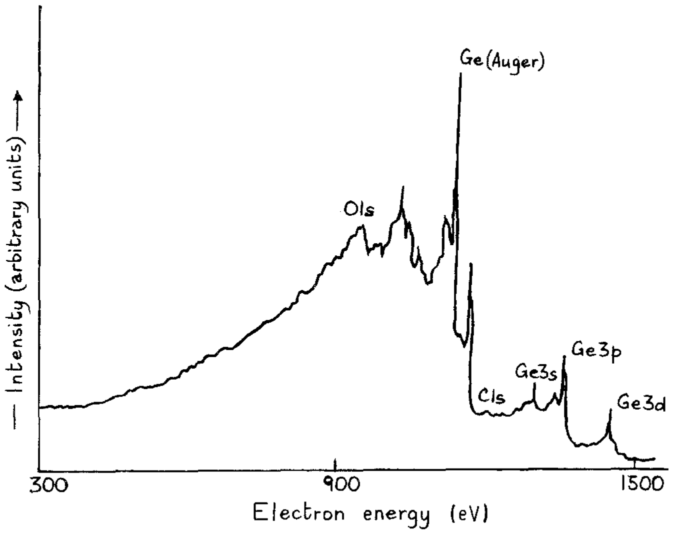

Figure 4 XPS spectrum of a GeO_x thin film deposited *in vacuo* at about 1.0 mPa.

doublet ($3d\ \frac{3}{2}$; $3d\ \frac{5}{2}$) at a binding energy of 29 eV with a small shoulder at 31 eV; the half-width is 1.7 eV. The effect of evaporating germanium at higher oxygen partial pressures can be observed in Fig. 5 in which the germanium 3d peak is shifted to smaller kinetic energies (or higher binding energies). Numerical values are presented in Table II, where, for example, at a partial pressure of 50 mPa, the germanium 3d main peak is centred at a binding energy of 31.1 eV, with the shoulder at 29.9 eV and the half-width covers a range of 3.6 eV. Also shown in Fig. 5 is the XPS spectrum of GeO_2. It consists of a single peak with a binding energy of 33.2 eV (Table II) which is in good agreement with the standard value of 33 eV [6].

5. Procedure for analysis of XPS data

The core energy levels of the units depicted in Fig. 2 are different, each being dependent on the degree of oxidation x. In order to relate these core level shifts with the environment of the atom an analysis based on electronegativity considerations is employed. There are several quantitative electronegativity scales but the one used here is due to Sanderson [7], as this technique provides a comparatively simple means of estimating atomic charges and calculating core level shifts.

The binding energies of the 3d electrons in the germanium atoms at the centres of the five different units illustrated in Fig. 1 were calculated in terms of the amount of oxygen x in the non-stoichiometric formula $-OGeO_x$. Denoting a $-GeO_x$ sub-unit by A, a $-Ge(GeO_x)_3$ sub-unit by B and an $-OGeO_x$ sub-unit by C, it is possible to calculate the electronegativities of the five sub-units in the following manner. The electronegativity of sub-unit A is given by

$$E_A = (E_{Ge}E_0)^{1/(1+x)} \qquad (1)$$

where E_{Ge} and E_0 are the electronegativities of germanium and oxygen on the Sanderson scale (E_{Ge} = 3.59; E_0 = 5.21). Similarly

$$E_B = (E_{Ge}E_A^3)^{1/4} \quad \text{and} \quad E_c = (E_{Ge}E_c^{1+x})^{1/(2+x)} \qquad (2)$$

E_A, E_B and E_c are, therefore, functions of x and vary monotonically as x varies from 0 to 2. The electronegativities of the five sub-units in Fig. 2 were calculated next using

$$E_i = E_{Ge}E_C^{5-i}E_B^{i-1} \quad i = 1, 2, \ldots, 5 \qquad (3)$$

and the binding energy of a 3d electron in a germanium atom, in eV, at the centre of any of the five sub-units is finally given by

$$BE(Ge^i) = 28.94 + 4.65\,(E_{Ge}^i - E_{Ge}) \qquad (4)$$

where the term in parentheses is the electronegativity difference between the ith germanium-containing unit and a germanium atom in the metallic state. Values of $BE(Ge^i)$ are shown in Fig. 6 as a function of x.

In order to simulate the XPS data: (i) it is assumed that the experimental germanium 3d peak is formed

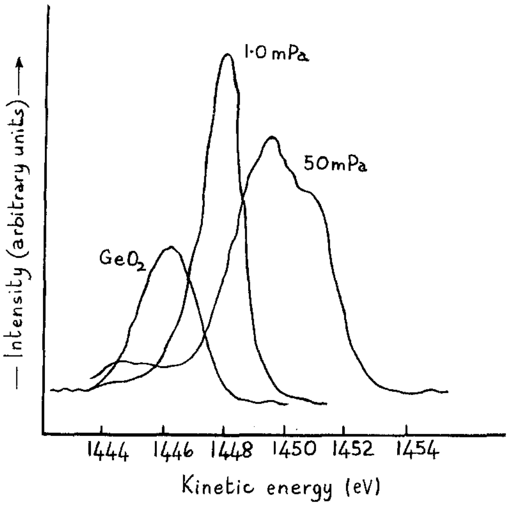

Figure 5 XPS spectra of the Ge 3d peak in GeO_x thin films prepared at two oxygen partial pressures compared with GeO_2.

TABLE II The shift in the O 1s and Ge 3d binding energies as a function of oxygen partial pressure

Oxygen partial pressure (mPa)	Oxygen binding energy (eV)	Germanium 3d	
		Binding energy (eV)	Base width (eV)
1.0	529.0	29.0	1.7
10.0	530.6	29.4	1.8
50.0	531.6	31.1; 29.9	3.5
90.0	–	31.9	4.5
GeO_2	532.1	33.2	2.55

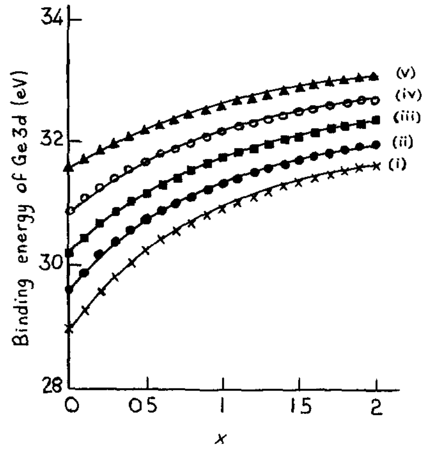

Figure 6 Calculated binding energies of the Ge 3d electron in the five sub-units as a function of the number fraction.

by the overlapping of the five subpeaks arising from each of the units in Fig. 2; (ii) the relative amounts of each of the five units as a function of x is known. Following Takano *et al.* [3] and Hübner [8] the probability of occurrence C_r of the five units may be expressed as

$$\begin{aligned} C_1 &= P^4(\text{Ge–O}) \\ C_2 &= 4P^1(\text{Ge–Ge})\,P^3(\text{Ge–O}) \\ C_3 &= 6P^2(\text{Ge–Ge})\,P^2(\text{Ge–O}) \qquad (5) \\ C_4 &= 4P^3(\text{Ge–Ge})\,P^1(\text{Ge–O}) \\ C_5 &= P^4(\text{Ge–Ge}) \end{aligned}$$

in which the probability of a Ge–O band in GeO_x is

$$P(\text{Ge–O}) = 2x/(2+x) \qquad (6)$$

and of a Ge–Ge bond is

$$P(\text{Ge–Ge}) = (2-x)/(2+x) \qquad (7)$$

Fig. 7 illustrates the results obtained for each of the units as a function of x, from which their distribution at different oxygen partial pressures can be obtained, see Table III.

XPS peaks, in general, may be modelled using appropriate admixtures of Gaussian and Lorentzian lineshape functions. The Gaussian parameter represents the combined resolution of the monochromator and the electron analyser of the spectrometer whereas the Lorentzian parameter depends on the lifetime of the hole generated when a 3d electron has been ejected by an incoming photon. Both parameters were varied until optimal agreement between experiment and theory was obtained. Using Fig. 7, sub-peaks corresponding to each of the units may now be determined and summed to yield the simulated XPS peak. In all cases the experimental line-shapes were found to be Gaussian.

TABLE III Distribution of the five sub-units at various oxygen partial pressures

	Oxygen partial pressures (mPa)					
Possible units	1.0	10.0	20.0	40.0	70.0	GeO_2
$Ge–O_4$	0	0	0	0.05	0.32	1.00
$Ge–GeO_3$	0	0	0.02	0.21	0.42	0
$Ge–Ge_2O_2$	0	0.04	0.13	0.37	0.21	0
$Ge–Ge_3O$	0	0.28	0.40	0.29	0.05	0
$Ge–Ge_4$	1.00	0.67	0.45	0.08	0	0

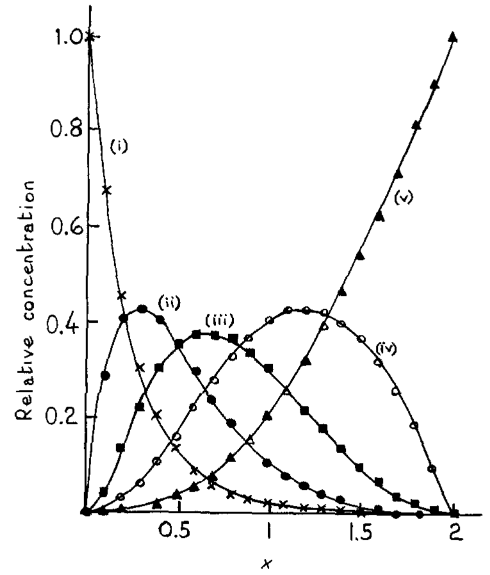

Figure 7 Calculated concentrations of the five sub-units as a function of the number fraction.

Fig. 8 depicts the peak value of the measured binding energy as a function of x. The total range of the chemical shift is 4.5 eV, which compares favourably with 4.7 eV [3] and 4.3 eV, the theoretical value obtained from Fig. 6. Fig. 9 illustrates representative plots of the five component Gaussians, together with their resultant, for x equal to 0.6.

6. Discussion

It must be noted that the optical and XPS techniques measure different quantities. The former measures the metallic volume fraction in the thin film and the latter the number fraction. These can be related, to some extent, if the volumes of the germanium and GeO_2 units in the cermet film are known. Complete agreement cannot be obtained because the calculations employed in the optical method is based on a two-component model whereas those in the XPS model are based on a five-component model. Table III indicates that moderate agreement is obtained for x nearly equal to 0 and 2. Large differences are present when x is about 1 for then the fundamental difference between the two techniques is at its greatest.

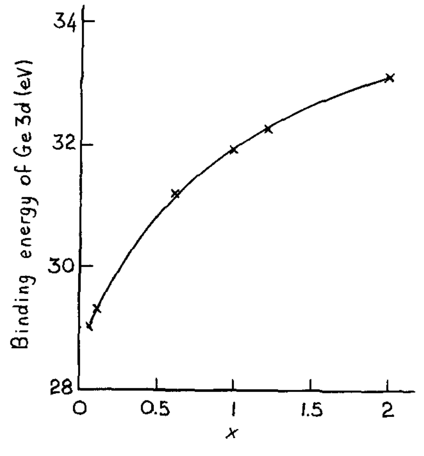

Figure 8 Peak value of the measured binding energy as a function of the number fraction.

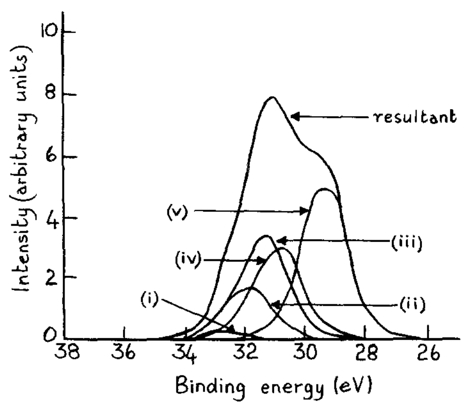

Figure 9 Simulated Ge 3d XPS peak for a $GeO_{0.6}$ thin film and the individual XPS curves for the five sub-units.

For simplicity, consider a binary system consisting of a mixture of germanium and GeO_2. The number fraction n of GeO_2 in GeO_x for XPS measurements is given by

$$n(GeO_2) = (x/2)/[(1 - x/2) + x/2] = x/2 \qquad (8)$$

and the number fraction of germanium in GeO_2 is given by

$$n(Ge) = 1 - x/2 \qquad (9)$$

The corresponding volume fractions V for the optical measurements are

$$V(GeO_x) = (x/2)/[(1 - x/2)V_{Ge}/V_{GeO_2} + (x/2)] \qquad (10)$$

and

$$V(Ge) = 1 - V(GeO_2) \qquad (11)$$

Here, V_{GeO_2} and V_{Ge}, respectively, are the effective volumes of the GeO_2 and germanium units in the cermet film.

If the ratio V_{Ge}/V_{GeO_2} is taken to be 0.18 then Table IV is obtained. It is now possible to relate V(Ge) to n(Ge) by comparing Tables I and IV. It can be seen, for example, that a V(Ge) of 0.29 corresponds to a n(Ge) of 0.7 when x is 0.6. Hence, we arrive at Table V for the complete range of oxygen partial pressures studied.

TABLE IV Comparison of V(Ge) and $V(GeO_2)$ with n(Ge) and $n(GeO_2)$ for various values of x in GeO_x (assuming a binary system of germanium and GeO_2).

Number fraction x	Optical		XPS	
	V(Ge)	$V(GeO_2)$	n(Ge)	$n(GeO_2)$
0.100	0.774	0.226	0.950	0.050
0.200	0.382	0.618	0.900	0.100
0.300	0.505	0.495	0.850	0.150
0.400	0.419	0.581	0.800	0.200
0.500	0.351	0.649	0.750	0.250
0.600	0.296	0.704	0.700	0.300
0.700	0.251	0.749	0.650	0.350
0.800	0.213	0.787	0.600	0.400
0.900	0.180	0.820	0.550	0.450
1.000	0.153	0.847	0.500	0.500
1.100	0.128	0.872	0.450	0.550
1.200	0.107	0.893	0.400	0.600
1.300	0.088	0.912	0.350	0.650
1.400	0.072	0.928	0.300	0.700
1.500	0.057	0.943	0.250	0.750
1.600	0.043	0.957	0.200	0.800
1.700	0.031	0.969	0.150	0.850
1.800	0.020	0.980	0.100	0.900
1.900	0.009	0.991	0.050	0.950
2.000	0	1.000	0	1.000

TABLE V Comparison of germanium volume fraction with germanium number fraction at various oxygen partial pressures

Oxygen partial pressure (mPa)	Germanium volume fraction (optical)	Germanium number fraction (XPS)
1.0	1.00	1.00
8.0	0.67	0.95
13.0	0.60	0.90
26.0	0.50	–
50.0	0.29	0.70
90.0	0.14	0.50
GeO_2	0.04	0.00

An estimate of the effective volume of germanium in the cermet may be obtained as follows: GeO_2 can exist either as a rutile structure of density $6.239\,g\,cm^{-3}$ with two GeO_2 units per unit cell or as a structure of lower density equal to $4.228\,g\,cm^{-3}$. Using this data, with the relative molar mass of GeO_2 we calculate the volume of the GeO_2 unit to be $2.78 \times 10^{-2}\,nm^3$ in the rutile form and $4.12 \times 10^{-2}\,nm^3$ in the less dense form. If the effective volume ratio of germanium to GeO_2 is taken to be 0.18, then the effective radius of germanium is obtained as 0.074 nm and 0.121 nm, respectively. The first value does not agree with that quoted in the literature [9], namely 0.122 nm, whereas the second value does.

7. Conclusions

Data obtained from optical transmission and XPS measurements have been used to determine the composition of GeO_x thin films. Although these techniques measure different quantities – the former the volume ratio of Ge : GeO_2 in GeO_x thin films and the latter the number fraction – it has been shown that the two sets of data can be correlated if: (a) an empirical value of 0.18 is used for the effective volume ratio of Ge : GeO_2; (b) the germanium dioxide is in its low density form. Such a result is not inconsistent with the amorphous nature of the thin films and the physical properties of germanium and GeO_2.

Note

A listing of the program in BBC Basic may be obtained from Dr E. L. Short.

Acknowledgements

One of us (M.M.S) wishes to thank the Egyptian Government for the award of a research scholarship.

References

1. H. BIREY, *J. Appl. Phys.* **45** (1974) 3946.
2. H. DEMIRYONT and N. TEZEY, *Thin Solid Films* **101** (1983) 345.
3. Y. TAKANO, Y. TANDOH, H. OZAKI and N. MORI, *Phys. Status Solidi* **130** (1985) 431.
4. J. C. CARVER, R. C. GRAY and D. M. HERCULES, *J. Amer. Chem. Soc.* **96** (1974) 6851.

5. R. C. GRAY and D. M. HERCULES, *J. Electron Spectrosc. Related Phenomena* **12** (1977) 37.
6. D. BRIGGS, "X-ray and Ultra-violet Photoelectron Spectroscopy" (Heyden, London, 1977).
7. R. T. SANDERSON, "Chemical Bonds and Bond Energy" (Academic Press, New York, 1971).
8. K. HÜBNER, *Phys. Status Solidi a* **61** (1980) 665.
9. "Handbook of Chemistry and Physics" (CRC Press, Cleveland, 1975).

Received 30 November 1987
and accepted 19 April 1988